

# Studies on Ionic Mass Transfer at Decreasing Coefficient Region on A Rotating Disc with Submerged Impinging Jet in A Closed Cell

P. King\*, V.S.R.K. Prasad and G. Hanumantha Rao

Department of Chemical Engineering  
Andhra University  
Visakhapatnam 530 003

Paper Received : 25.5.06

Revised Paper Accepted : 19.7.06

*The mass transfer studies at decreasing coefficient region on a rotating disc with submerged impinging jet in a closed cell were carried out in the present work. The limiting current technique for reduction of ferricyanide ion was employed. For varying parameters like nozzle sizes, rotational speeds, the experimental mass transfer data were analyzed and correlated for two ranges of heights from target surface,  $H_n = 0.05$  m and  $H_n > 0.05$  m. The mass transfer coefficients were increased with increase in flow rate and were also increased with increase in nozzle diameter at any given velocity. The coefficients were linearly decreased with increase in the distance between the nozzle end and the rotating disc surface. For a six fold increase in the rotational speeds, the improvements in the coefficients were about 38 per cent.*

Several augmentation techniques have been in practice for the enhancement of heat and mass transfer coefficients. Of these techniques, majority of the forced convective conditions have been induced in the form of (i) agitation / stirring of the fluid, (ii) using an impinging-jet flow of the fluid on the reacting surface 'stationary or rotating', (iii) using divergent and convergent sections, (iv) vibration or rotation of the reacting surface (electrode surface), (v) generating high turbulent conditions near the reacting surface by inserting promoters of different geometries, and, (vi) fluidization, in which the fluidizing solids fraction greatly affects the transfer coefficients at the reacting surface. Among these, impinging jet is attracting the researchers in view of its industrial applications, such as, heating, cooling, and deposition of mass at large surface area. Besides these, they find application in electrochemical processes for rapid removal of heat, electrochemical surface treatment of selective areas (say anodizing or the processing of

printed circuit boards), annealing of metals and plastic sheets, tempering of glass, drying of textiles, veneer and film materials, etc. The impinging jets hitherto employed are broadly classified as (i) free jets, and, (ii) submerged jets.

A new investigating method has been introduced by Frumkin and Nekrasov [1] where the target surface, over which an electrochemical redox reaction occurs, is rotated and a multifold increase in the rates is observed when the fluid interacts with the surface in the form of an impinging jet. The rotating disc electrode system has been found to be more efficient system for obtaining better mass transfer coefficients and it has certain additional advantages over other geometries wherein one needs a very simple experimental setup. A three-dimensional boundary layer flow over a uniformly accessible surface has been identified. The benefits of rotating disc electrode are: (i) a diffusion layer is developed with a thickness that does not change with time; (ii) double layer charging has a minimal effect on the measurement; (iii) stable and laminar flow is ensured over a wide range of operating conditions; (iv) the current, potential and fluid-flow characteristics are well established; (v) uniform limiting current densities can be obtained; (vi) construction and operation of the rotating disc electrodes are easier and offer unique characteristics, especially for mechanistic investigations; (vii) the devices are commercially available; (viii) the relatively low rate of mass transfer to a rotating disc electrode restricts current requirements to a low level allowing the use of modest power supplies; (ix) the theoretical basis of the mass transfer process is solved and equations are available to relate the experimental parameters to the mass transfer at the electrode surface.

---

\* Author for correspondence  
E-mail : P\_king@rediffmail.com

In the literature, most of the work have been confined to free jets and relatively a few investigations have been carried out with submerged jets in open cells. The present work is aimed at studying the mass transfer coefficients with submerged jets on to a rotating target surface in a closed cell. Most of the operations are to take place in closed containers. This work helps in providing data for mass transfer coefficients in closed cells.

Thus, the present study is directed towards the investigations on mass transfer with impinging jets in closed containers in the presence of rotation of the target surface.

Several experimental systems relating to mass transfer from rotating bodies in axisymmetric flow have been reported in literature [2-4]. Several investigators utilized the impinging jet system for electrochemical studies [5-10]. Chin and Tsang [7] presented both the theoretical and experimental studies of mass transfer at a circular disc electrode in the stagnation region of an impinging jet. Chin and Chandran [8] extended the study to a ring disc electrode and set a trend to develop the impinging jet as a practical tool for electro analytical applications. Alkire and Chin [9] utilized an unsubmerged jet system to study high speed selective electroplating. Mass transfer measurements were carried out in the impingement region by using disc electrodes of different radii and in the wall jet region by using a sectioned electrode respectively. Mass transfer from a rotating disc imposed by an external forced flow was studied by Shi-Chern-Yen et al. [10]. The experimental mass transfer rates were measured by the electrochemical method. The complementary characteristics of the rotating disc electrode and rotating cylinder electrode have been compiled in the literature [11-14]. Numerical solutions [15,16] were obtained for heat transfer using coaxial rotating discs and for radial through-flow between a stationary and rotating disc. A review on heat transfer was presented by Eckert et al. [17]. Both theoretical and experimental results were compiled in his review work.

### Experimental Setup and Procedure

The schematic diagram of the equipment used in the present study is the same as that described elsewhere [10,18]. The experimental unit mainly consisted of a copper storage tank, a pump, a rotameter, a test cell and a motor-driven pulley system for varying the rotational speeds. A coil with perforations is placed inside the tank for deaeration of electrolyte by bubbling nitrogen through the perforations whenever required. The electrolyte from the storage tank was circulated through rotameter and the test cell.

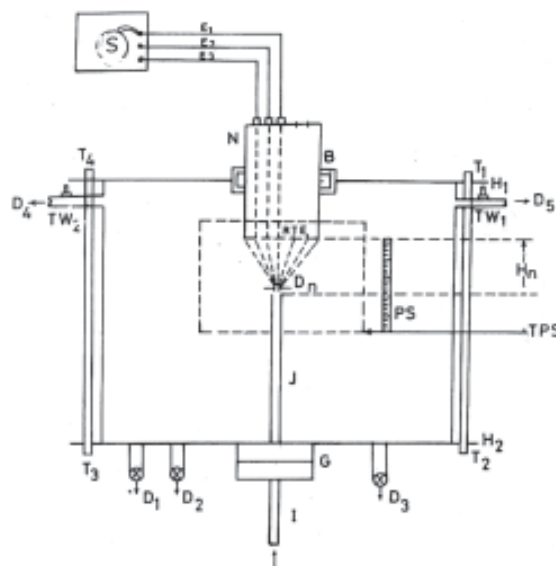


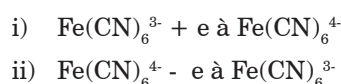
Fig. 1

The test cell consisted of an electrolytic cell made out of cylindrical PVC section closed on either ends ( $H_1, H_2$ ), an electrode assembly and a motor driven pulley system. The test cell is shown in Fig.1. A pointer scale (PS) attached to the nozzle from assembly (shown in Fig.1) facilitated the measurement of distance of the nozzle from the bottom end, and, hence, the distance between the target surface containing the test electrodes and the nozzle-end ( $H_n$ ). Provision was made to ensure that during experimentation electrode assembly was fully submerged in the electrolyte. A transparent Perspex strip (TPS) fixed to the cell body served as a window to observe the fluid movements inside the electrolytic cell. A thermometer having a temperature range from 0-100°C was used to measure the temperature of the recirculating fluid electrolyte in the cell upto 0.1°C accuracy. Two thermo-wells ( $TW_1$  and  $TW_2$ ) were provided at the top exit end of the test cell (as shown in the Fig. 1) to indicate the temperature of the electrolyte in the cell.

The test electrode assembly consisted of a nylon rod (N), cylindrical, cut to the size from a 4.5 cm dia rod section and machined to the required dimensions. Three test electrodes made of copper fixed equidistant flush with the bottom end surface of the cylindrical nylon rod served as the target surface. The central electrode was disc type with a diameter of 0.6 cm while the other two were ring type at distances 1.4cm and 2.7cm respectively, from the centre point of the target surface. A similar set of three electrodes were fixed flush with the top end surface of the nylon rod. The nylon rod with its electrode assembly was mounted on ball bearings (B)

over which it could freely rotate and fixed to the top hylam flange plate of the test cell ( $H_1$ ). The other end, projected outward, was linked to a motor-driven pulley system. The motor-driven pulley system was of Vickson type and rested against a rigid concrete pillar. The speed of the rotating target surface was measured by a tachometer. The rotameter was calibrated prior to the commencement of the experimental run. Thin copper rods riveted to the copper electrodes at the top end-surface and drawn to the bottom-end surface, provided electrical connection between carbon brushes used for electrical contact on rotation and the concentric copper electrodes fixed flush with the bottom-end surface (target surface). The selector switch (S) facilitated to obtain the limiting current measurements at any desired electrode.

Cathodium reduction of ferricyanide ion and anodic oxidation of ferrocyanide ion in the presence of excess indifferent electrolyte can be represented as



The electrolyte consisted of equimolar solutions of 0.01 M potassium ferricyanide and potassium ferrocyanide with an indifferent electrolyte 0.5 N sodium hydroxide. All the test electrodes were polished with zero emery paper and their surfaces were degreased by chemical solvent treatment. For each flow rate, the recirculation of the electrolyte was allowed till the flow rate and the temperature of the electrolyte were stabilized. The method employed to obtain the limiting current data was similar to those reported earlier [19-21]. This method dispensed with the use of any standard reference electrode as :

- The area of the test electrode was so small compared to the counter electrode that a constant potential at the latter could be established.
- The values of limiting current densities were only relevant to evaluate mass transfer coefficients and the actual values of electrode potential were not required in the present study, and,
- The values of the limiting currents obtained by the method described above were nearly the same as those obtained by using standard calomel reference electrode.

In the present study, limiting current measurements were made for the case of the forced convective jet flow in the presence of rotation of the target surface containing the test electrodes. The mass transfer coefficients were calculated by  $k_L = i_L / nAFC_o$ , where  $i_L/A$  (amp/m<sup>2</sup>) was the limiting current density. The diameter, distance of the nozzle and speed of the rotating target surface were varied and experiments were repeated for each case. The temperature of the electrolyte was noted for each run. The concentration of the reacting ion for each run was estimated using titrometric methods. The concentration of ferricyanide ion was estimated using idometric titration [22-23] while that of ferrocyanide ion was estimated by using permanganometry [22].

### Result and Discussions

The parameters studied, the range of the parameters covered are compiled in Table 1. The data on limiting current densities, for the case of reduction of ferricyanide ion obtained at the three electrodes E1, E2, E3, fixed flush with the surface of the rotating disc are plotted against  $(1+r_e)$  where  $r_e$  is the radial distance of the electrode, as shown in Figs 2 to 5. The data in all these cases showed a maximum value of the coefficient at the electrode on which the jet directly impinges and the coefficient steeply declines initially with increase in the radial distance from the point of impingement. It appears, as the radial distance tends to approach the wall of the container, the decrease is found to be gradual and the values of the coefficients remain nearly constant. An asymptotic approach of the coefficients to a minimum, as  $r_e$  approaches the radius of the rotating

**Table 1: Range of Variables Covered in the Present Study**

Variable	Minimum	Maximum	Max/Min
Flow rate, $(Q \times 10^5) \text{ m}^3/\text{s}$	4.5	31	6.89
Velocity, $V_n$ m/s	0.147	13.92	94.694
Distance of the nozzle from target surface $(H_n \times 10^2)$ , m	1.0	9.0	9.0
Diameter of the nozzle $(D_n \times 10^3)$ , m	4.0	9.0	2.25
Reynolds Number, $(Re_n)$	3404	69104	20.3
Rotational Reynolds Number $(Re_r)$	28	14823	529.393
Schmidt Number, $(Sc)$	739	1063	1.438
Froude Number, $(Fr)$	0.1	4943	49430
RPM of the target surface	106	680	6.415

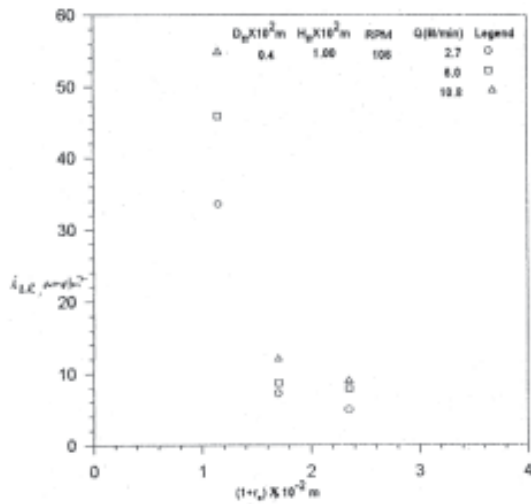


Fig. 2 : Variation Limiting Current Densities with  $(1+r_s)$  at Various Flow Rates

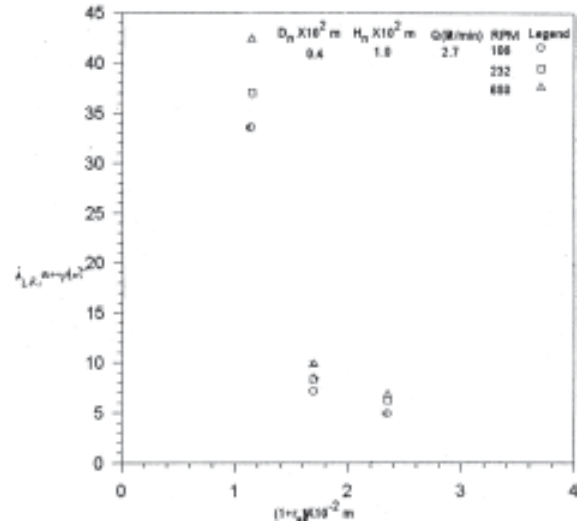


Fig. 5 : Variation Limiting Current Densities with  $(1+r_s)$  at Various Speeds

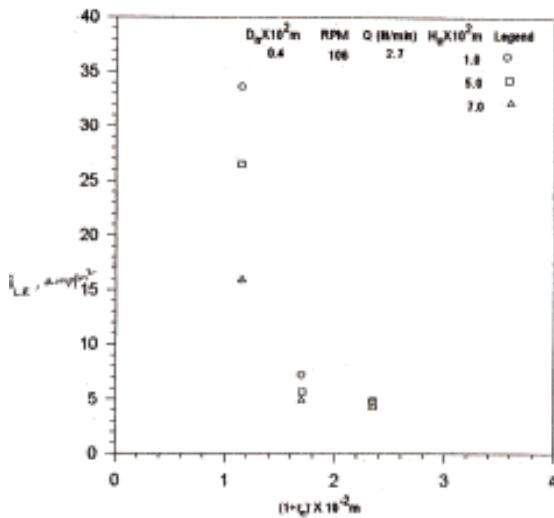


Fig. 3 : Variation Limiting Current Densities with  $(1+r_s)$  at Various Nozzle Distances

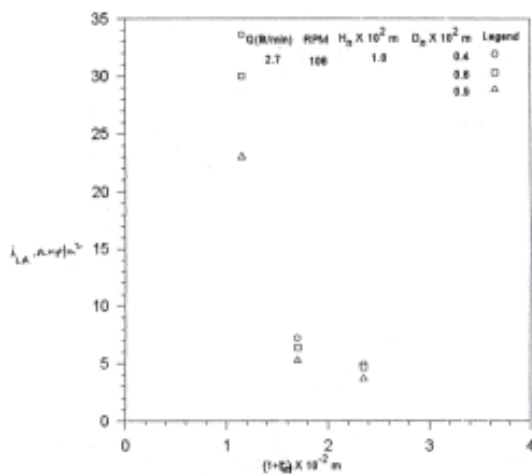


Fig. 4 : Variation Limiting Current Densities with  $(1+r_s)$  at Various Nozzle Sizes

disc is an indication of gradual dissipation of fluid turbulence radially towards the edge of the rotating disc.

The impinging jet onto a target surface makes a bell shape of exit flow. But in the upward impingement, there is a possibility of the outer layers of the bell pulled down due to gravity, and, hence, a sudden decrease in coefficient might have resulted with a small increments from the point of impingement. The regions identified from the above figures are defined as follows:

- (i) Impingement region: Wherein the coefficients are maximum and decline rapidly as we move away from this region.
- (ii) Decreasing coefficient region: Wherein the coefficients are much lower compared to those in impingement region and the decrease in the coefficient with increase in the radial distance of the electrode is found to be marginal.

The two regions can be further characterized by the dimensionless distance parameter  $\ddot{a}$  defined as  $\ddot{a} = r_e / (D_r/2)$ .

Plot of mass transfer coefficients against  $(1+\ddot{a})$  is shown in Fig. 6 for the data obtained with  $D_n = 0.004\text{m}$ ,  $0.006\text{m}$  and  $0.009\text{m}$  at constant height of the nozzle ( $H_n = 0.01\text{m}$ ). The coefficients are found to be maximum at  $(1+\ddot{a}) = 1.067$ . For all nozzle sizes used in the present study, the coefficients are found to decline rapidly upto  $(1+\ddot{a}) = 1.311$ , and, thereafter, decrease gradually.

The data on coefficients hitherto shown in the plot (Fig. 6) also reveal two different regions which can be characterized by the dimensionless distance parameter  $(1+\ddot{a})$  as:

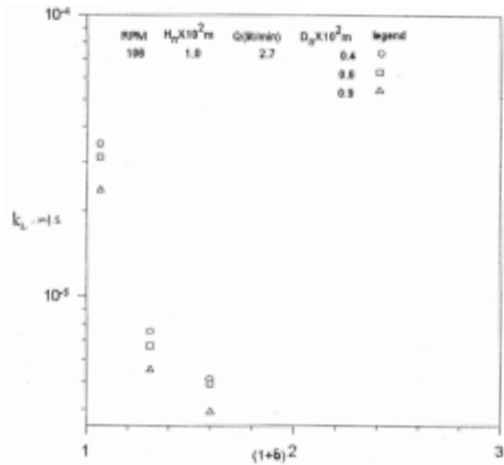


Fig. 6 : Variation of Mass Transfer Coefficient with  $(1+\delta)$

Impingement region:  $(1+\delta) < 1.311$   
 Decreasing coefficient region :  $(1+\delta) \geq 1.311$

The entire experimental data on mass transfer is analyzed for decreasing coefficient region only to evaluate the effects of other pertinent variables and to develop generalized correlations.

**Effect of Nozzle Distance from the Rotating Disc**

The plots of the data for mass transfer for reduction of ferricyanide ion against velocity in the decreasing coefficient region with the nozzle dia of 0.004 m located at various distances ( $H_n$  varying from 0.01m

to 0.09m) and at fixed RPM (=232) are shown in Fig. 7. The plot shows a marginal decrease in the coefficients upto a nozzle distance of 0.05m and decline rapidly thereafter. In general, in submerged jets, an increase in the distance of the nozzle from the target surface increase the static liquid head above the nozzle end, thus resulting in lower coefficients. In case of submerged jets, with the jet issuing out of the nozzle in the upward direction, the intensity of impinging flow is further reduced, most probably due to an additional component of gravitational force, pulling the up-flowing jet downwards. Both considerably decrease the coefficients when  $H_n$  is increased. This effect is shown as cross plot in the in-set of Fig.7. Thus, the data in this region are further divided into two regions:

- i)  $H_n = 0.05$ m
- ii)  $H_n > 0.05$ m

Similar division was reported even in earlier studies [18] for variation of nozzle distance from the target surface:

**Effect of Nozzle Diameter**

For a given velocity, as the diameter of nozzle is increased, the turbulence increases. Intensity of impingement at the target surface is also likely to increase, and, thus, contributes much to the enhancement of coefficients. The shearing effect of

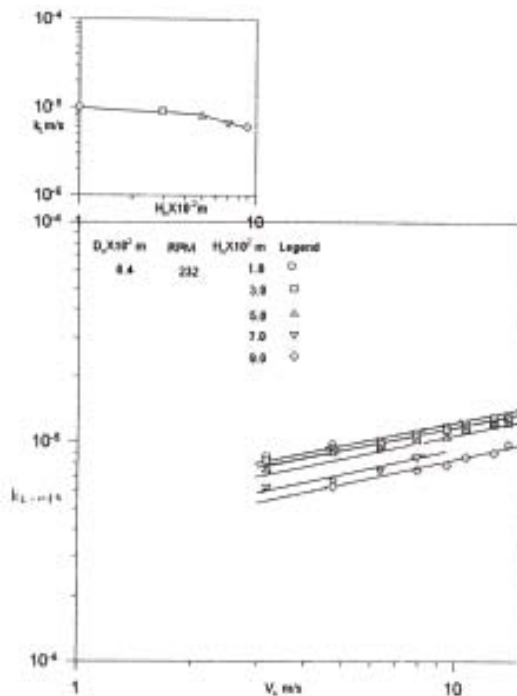


Fig. 7 : Variation of Mass Transfer Coefficient with Velocity in Decreasing Coefficient Region (E2)

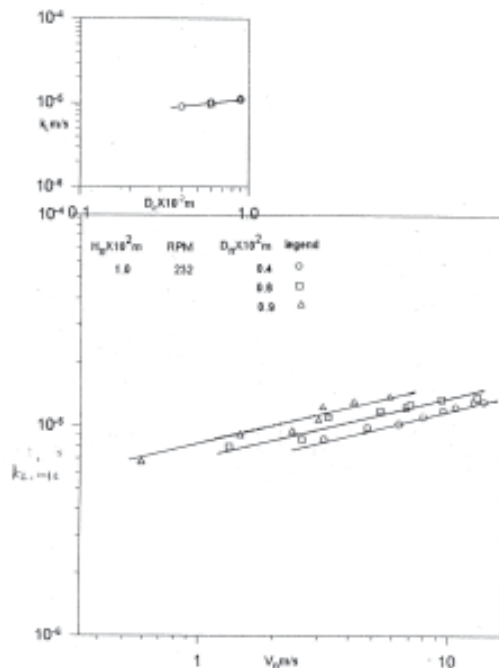
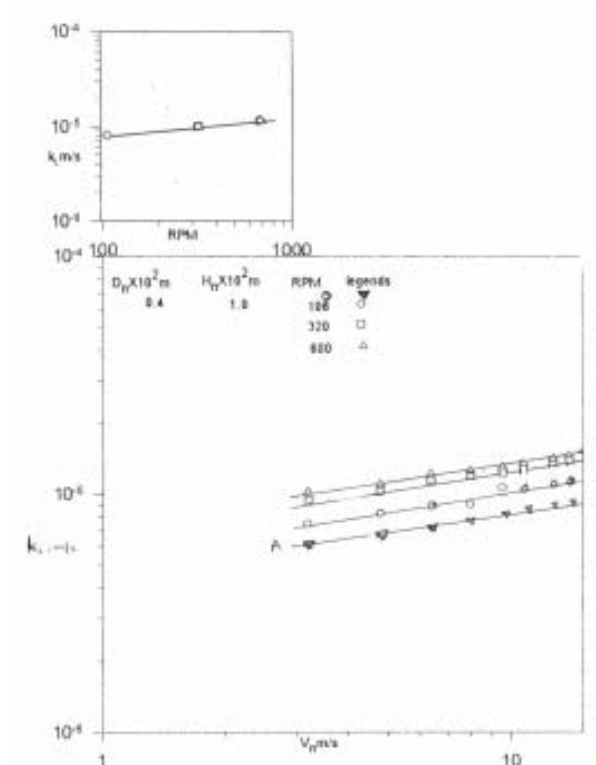


Fig. 8 : Variation of Mass Transfer Coefficient with Velocity at Various Nozzle Sizes in Decreasing Coefficient Region (E2)



**Fig. 9 : Variation of Mass Transfer Coefficient with Velocity at Various Speeds in Decreasing Coefficient Region (E2)**

the rotating disc further augments the coefficients. These effects are shown in Fig. 8. The variations of mass transfer coefficients with  $D_n$  are shown as cross plot as inset of Fig. 8. For a 2.25 fold increase in nozzle diameter, the improvements are found to be upto 39%.

**Effect of Rotational Speed of the Target Surface**

The rotation of target surface containing the electrode has two-fold effect.

1. Causing effective churning of the liquid electrolyte flowing through the electrolytic cell.
2. Causing effective dispersion of the impinging fluid electrolyte.

The rotating target surface effectively shears the impinging fluid, resulting in rigorous mixing of the fluid elements in the vicinity of the electrode surface. The combined effect of the above two lead to significant improvement in coefficients. The data on  $k_L$  for all rotational speeds for the case of  $D_n = 0.004$  m and  $H_n = 0.01$ m and 0.07m are plotted in Fig. 9. Plot A in Fig. 9 gives the data on  $k_L$  plotted against velocity in the absence of rotation. The augmentation is comparable within the range of rotational speeds employed and the improvements range from 2-12 fold. It may be concluded that within

the range of rotational speeds used, the coefficients increase markedly with the increase in RPM. The improvements in the coefficients with rotation are about 1.4 times to those in the absence of rotation (plot A).

For a six-fold increase in the rotational speeds, the improvements in the coefficients are upto 38 percent. The improvements in coefficients due to rotation range from 14 ( at the minimum RPM) to 57 percent (at the maximum RPM).

**Development of Generalized Correlations**

The rotating disc imparts circulatory flow-patterns within the flowing fluid electrolyte by generating a vortex flow in the core of the bulk fluid electrolyte. The impact of the centrifugal action of rotating liquid column may be very much seen on the walls of the closed container cell. However, its effect on the electrodes in the present case cannot be undermined in view of the churning action induced by the rotating disc. Hence, it is contemplated that a better representation of the data could be obtained by introducing the Froude group ( $V_n^2 / D_n g_c$ ) where  $V_n^2 / g_c$  will take sufficient care of the effects due to the rotation of the target surface. Prasad [18] in his studies on submerged jets, correlated the data employing Fr as one of the dynamic dimensionless parameters which in his case yielded low average and standard deviations.

Correlations were developed by incorporating the radial velocity component in Fr,  $Re_r$  and  $J_D$  factors. On regression analysis, the data on reduction of ferricyanide ion yielded the following correlation with low standard deviation shown against each correlation.

For  $H_n = 0.05$ m

$$J_D = 0.7241 \times 10^{-3} (Fr)^{-0.3374} (Re_r)^{0.211} (H_n / D_n)^{-0.03916} (1 + \delta)^{-2.724} \text{ Std.deviation: 10.2\%}$$

For  $H_n > 0.05$ m

$$J_D = 0.4611 (Fr)^{-0.3157} (Re_r)^{0.2762} (H_n / D_n)^{-0.1459} (1 + \delta)^{-2.184} \text{ Std.deviation: 10.6\%}$$

**Conclusion**

Based on the limiting current density measurements, the conclusions drawn from these studies are as follow:

1. The coefficients are found to increase with the increase in flow rate (Q).
2. The coefficients are found to increase with an increase in the nozzle diameter  $D_n$  at any given velocity.
3. The coefficient linearly decrease with increase in

the distance between the nozzle end and the rotating disc surface. However, the decrease is found to be marginal upto a certain value of  $H_n \leq 0.05m$  and, thereafter, decline rapidly. The effects of variation in  $H_n$  on the coefficients have shown two distinct regions, one for the case of  $H_n \leq 0.05m$  and the other for  $H_n > 0.05m$ .

- Improvements in the coefficients of the present study over the empty conduit flow are very significant. A sevenfold increase in the flow rate ( $Q$ ) result in 100 – 500 fold increase in the coefficients.
- The improvements in the coefficients with rotation are about 1.4 times to those in the absence of rotation. For a six fold increase in the rotational speeds, the improvements in the coefficients are about 38 percent.

#### References

- Frumkin, A.N., and Nekrasov, L.V.: *Doklady Akad. Nauk. SSSR*, 126,115(1959).
- Sparrow, E.M., and Gregg, J. L.: *J. of Heat Transfer*, Trans. ASME.Series C., 82,294(1960).
- Subramanian, V., Krishna, M.S., and Adivarahan, P.: *Indian Journal of Technology*, 4,353, (1996).
- Krishna, M. S., Ramaraju, C.V., Jagannadharaju, G.J.V., and Venkata Rao, C.: *Indian Journal of Technology*, 6(2),50, (1968).
- Yamada, J., and Matsuda, H.: *J. Electroanal. Chem.*, 44,189 (1973).
- Coeuret, F., *Chem. Eng. Sci.*, 30, 1257, (1975).
- Chin, D.T., and Tsang, C.H.: *J. Electrochem. Soc.*, 125,1461, (1978).
- Chin, D.T., and Chandran, R.R., *J. Electrochem. Soc.*, 128,1904(1981).
- Alkire, R.C., and Chen, T.J.: *J. Electrochem. Soc.*, 129,2424(1981).
- Yen, S.C., Wang, J.S., and Chapman, T.W.: *J. of Electrochem. Soc.*, 139(8),2231 (1992).
- Gabe, D.R., Wilcox, G.D., J. Gonza Leg – Garlia and Walsh, F.C.: *J. of Applied. Electrochem.*, 28,759, (1998).
- Sobolik, V., Benabes, B., and Cognet, G., *J. of Appl. Electrochem.*, 25,441 (1995).
- Masse, N., St.Pierre, J., and Besereer., *J. Appl. Electrochem.*, 25,340(1995).
- Gabe, D.R.: *Chemical Abstracts.*, 123, (1995).
- Schmidt, R.R., and Patel, P, J.: *of Heat and Mass Transfer*, Trans. ASME., 117(1),79, (1995).
- Soong, C.Y., and Ma, H.L.: *Int. J. of Heat and Mass Transfer*, 38(10),1865 (1995).
- Eckert, E.R.G., Goldstein, R.J., Ibele, W.E., Patankar, S.V., Simon, T.W., Strykowski, P.J., Tamma, K.K., Knehn, T.H., Bar, A., Cohern, Heberlein, J.V.R., Davidson, T.J., Bischof, J., Kulacki, F., and Kortshagen, U., : *Int. J. of Heat and Mass Transfer.*, 42,2717, (1999).
- Prasad, V.S.R.K., Studies on Ionic Mass Transfer with Submerged Impinging Jets in Closed Cells, Ph.D. Thesis, Andhra University, Visakhapatnam, India (1994).
- Reiss L.P and Hanrathy, T.J, : *Amer. Inst. Chem. Engrs. J1.*, 245, (1962).
- Krishna, M.S., Raju, G.J.V.J., and Rao, Venkata, C.: *Indian Journal of Technology.*, 4, 8(1966).
- Sudhakara Rao, K., Ramaraju, C.V., and Raju, G.J.V.J.: *Indian Journal of Technology*, 6, 129(1966).
- Kolthoff, I.H., and Furman, N.H.: *Volumetric Analysis*, II, 427, John Wiley and Sons Inc, New York(1935).
- Sutton, F., : *Volumetric Analysis*, Blackisten & Co., Ohiladelphia ,235(1935).

#### Nomenclature

A	Surface area of electrode, m <sup>2</sup>
B	Bearing.
C <sub>o</sub>	Concentration of ferricyanide ion, kmol/cc.
D <sub>n</sub>	Diameter of the nozzle, m
D <sub>r</sub>	Diameter of the Nylon rod, m
D <sub>1</sub> – D <sub>5</sub>	Outlets of electrolyte from cell.
D <sub>L</sub>	Diffusivity of reacting ion, m <sup>2</sup> /s
E <sub>1</sub> -E <sub>3</sub>	Electrodes.
F	Faraday equivalent, Coulombs/equivalent.
G	Gland nut.
H <sub>n</sub>	Distance of the nozzle from the target surface, m
H <sub>1</sub> &H <sub>2</sub>	Hylam plates.
I	Inlet tube for electrolyte into the cell.
i <sub>L</sub>	Limiting current, amp.
i <sub>LR</sub>	Limiting current density, amp/m <sup>2</sup> .
J	Jet nozzles.
k <sub>L</sub>	Mass transfer coefficient, m/s.
n	Number of electrons per ion reacted at surface.
N	Nylon rod.
PS	Pointer scale.
RTE	Concentric ring electrodes on the target surface.
RPM	Speed of the rotating disc, rev/ min.
r <sub>e</sub>	Average radius of the electrode on the target surface, m.
S	Selector switch.
T <sub>1</sub> – T <sub>4</sub>	Tie rods.
TW <sub>1</sub> & TW <sub>2</sub>	Thermo wells.
TPS	Transparent Perspex sheet.
V <sub>n</sub>	Velocity of the Nozzle, m/s.

#### Greek letters :

$\rho$	Density of the electrolytic solution, kg/m <sup>3</sup>
$\mu$	Viscosity of the electrolytic solution, kg/m
$\omega$	Angular velocity, $2\pi$ (RPM) / 60, rad/s

#### Dimensionless Groups

Re <sub>n</sub>	Reynolds number ( $\bar{n} V_n D_n / \nu$ )
Re <sub>r</sub>	Rotational Reynolds number ( $\bar{\omega} r_e^2 \bar{n} / \nu$ )
Sc	Schmidt number ( $\nu / \bar{n} D_L$ )
Fr	Froude number ( $V_n^2 / g_c D_n$ )
J <sub>D</sub>	Mass transfer factor [ $(k_L / V_n) Sc^{2/3}$ ]